Aerodynamic Phenomena of Retro Propulsion Descent and Landing Configurations

Ansgar Marwege[1], Christian Hantz[1], Daniel Kirchheck[1], Josef Klevanski[1], Jan Vos[3], Mariasole Laureti[2], Sebastian Karl[2], Ali Gülhan[1]

[1]*DLR Institute of Aerodynamics and Flow Technology,*
Supersonic and Hypersonic Technologies Department, Linder Hoehe, 51147 Cologne, Germany

[2]*DLR Institute of Aerodynamics and Flow Technology,*
Spacecraft Department, Bunsenstrasse 10, 37073 Göttingen, Germany

[3]*CFS Engineering, EPFL Innovation Park, Batiment-A, 1015 Lausanne, Switzerland*

ABSTRACT

The RETALT (RETro propulsion Assisted Landing Technologies) project aims to investigate vertically landing launcher configurations, which decelerate by means of retro propulsion manoeuvres during the descent and final landing phase. One key objective was to understand the complex steady and unsteady flow field and the resulting oscillating pressure loads on the re-entering vehicles.
In the course of the project, extensive wind tunnel test series have been performed in the three aerodynamic wind tunnel facilities at DLR in Cologne. The re-entry burn, with one to three active engines, was rebuilt in the Hypersonic Wind Tunnel Cologne (H2K), the aerodynamic descent phase was analysed in the Trisonic Wind Tunnel Cologne (TMK) and the landing burn was tested in the Vertical Free-jet Facility (VMK). Furthermore, detailed CFD analyses of the various flight phases have been performed by CFSE and DLR with the flow solvers NSMB and TAU.
In this paper the steady and unsteady flow field around the RETALT1 and RETALT2 vehicles in the various flight phases will be compared and the resulting loads will be analysed.
An analytical sizing method for aerodynamic control surfaces for the aerodynamic phase of RETALT1 is validated, for RETALT2 a strong hysteresis was found in the forces and moments in the aerodynamic phase. The plume length in the landing phase of RETALT1 follows a linear analytical approach. The flow field of RETALT1 in the retro propulsion phases during the landing burn and the re-entry burn is highly unsteady which is visible in the variance of the schlieren images and in the high frequency pressure measurements.

Index Terms *— Retro Propulsion, Vertical Take-off Vertical Landing Technologies, Wind Tunnel Experiments, RETALT, Retro Propulsion Assisted Landing Technologies*

1. INTRODUCTION

In the RETALT (RETro propulsion Assisted Landing Technologies) project key technologies for the vertical descent and landing of launcher configurations with the aid of retro propulsion are investigated. An overview of the project is given in [1], [2] and [3].
One of the key technologies studied are the aerodynamics and aerothermodynamics of these configurations. These were studied for two configurations, RETALT1 and RETALT2. RETALT1 is a heavy lift launch vehicle with up to 14 t GTO payload capability (see Fig. 6). For this configuration the first stage is recovered with retro-propulsive vertical landing.
RETALT2 is a Single Stage to Orbit (SSTO) configuration with 500 kg to LEO (see Fig. 2). While RETALT1 is considered to be a configuration close to a Reusable Launch Vehicle (RLV), feasible in Europe in the medium-term, RETALT2 is more considered as a technology test bed configuration.
The two configurations were tested in four test facilities at the Supersonic and Hypersonic Technologies Department at DLR in Cologne. The Wind Tunnel facilities mapped onto the reference trajectory presented in [1] and [4] for RETALT1 is shown in Fig. 3. The different flight phases of RETALT1 are rebuild as follows. The re-entry burn with one or three active engines was rebuilt with cold gas air and with heated air in the Hypersonic Wind Tunnel Cologne (H2K). The aerodynamic phase with no active engines was rebuilt in the Trisonic Wind Tunnel Cologne (TMK) and the landing burn with the final touch down is simulated in the Vertical Free-Jet Facility Cologne (VMK), where cold gas and hot combustion of gaseous oxygen and hydrogen are used for the simulation of the exhaust plume. Material tests of the cork based TPS material developed by Amorim Cork Composites in the project were performed in the Arc Heated Facility L2K and are presented in [5].
Fig. 4 shows the wind tunnel facilities mapped on the reference trajectory of RETALT2 presented in [1]. For RETALT2 no re-entry burn is performed. The deceleration of the vehicle in the atmosphere is performed purely aerodynamically with the aid of a large capsule like base area. Finally, the landing burn is performed shortly before touchdown. The aerodynamic phase was tested in the TMK.
In Fig. 5 and Fig. 6 the Reynolds numbers tested in the TMK for RETALT1 and RETALT2 are compared to the flight conditions in the reference trajectory. For RETALT1 the Reynolds numbers are one order of magnitude lower in the TMK than in flight. As the flight points rebuilt for RETALT2 are still in relatively high altitudes, for RETALT2 the Reynolds numbers are matched well. Only for the subsonic Mach number tested (0.6) the Reynolds number in the TMK is one order of magnitude smaller than in flight.
In this paper a summary of findings for the different flight phases for RETALT1 and RETALT2 will be given. First the purely aerodynamic phases of RETALT and RETALT2 tested in the TMK will be discussed. Then, the phases with active retro propulsion for RETALT1 will be analyzed, namely the landing burn tested in the VMK and the re-entry burn tested in the H2K.

2. AERODYNAMIC DATA BASE

In the RETALT project extensive data bases of aerodynamic force and moment coefficients have been generated for the RETALT1 and the RETALT2 configurations. The data is published along with additional explanations and plots of the data in the Aerodynamic Data Base, AEDB2.0, for RETALT1 in [6] and for RETALT2 in [7].

a) Configuration with Petals during descent

b) Configuration with planar fins during descent

c) Configuration with folded planar fins during ascent

Fig. 1: RETALT1 configuration [3]

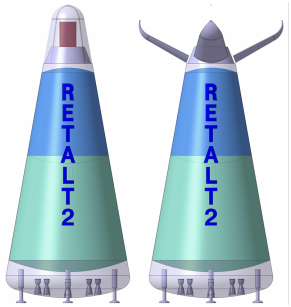

Fig. 2: RETALT2 configuration [1]

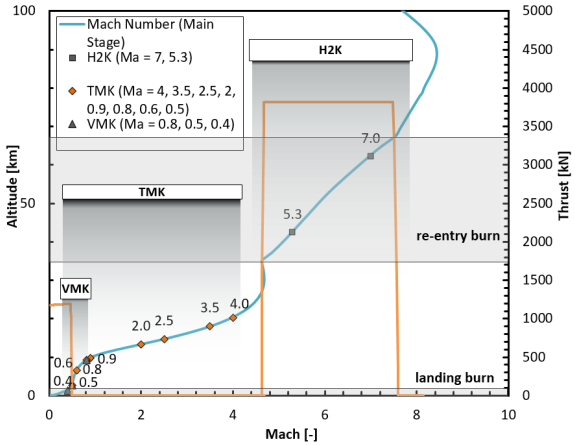

Fig. 3: Wind Tunnel Test Facilities mapped on RETALT1 reference trajectory [3]

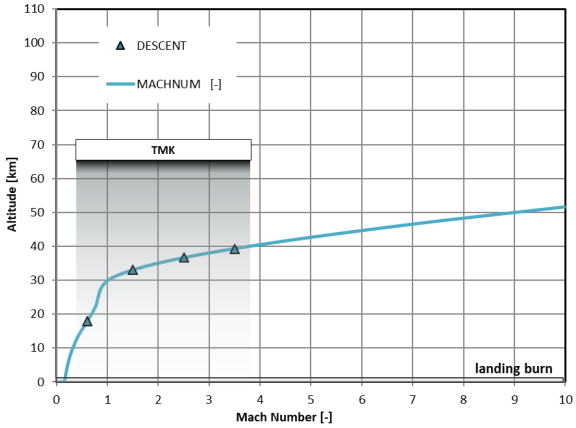

Fig. 4: Tests in TMK Test Facility mapped on reference trajectory presented in [1]

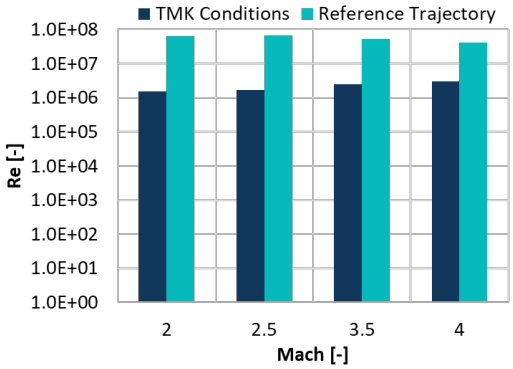

Fig. 5: RETALT1 comparison of Reynolds numbers in TMK tests and in flight [4]

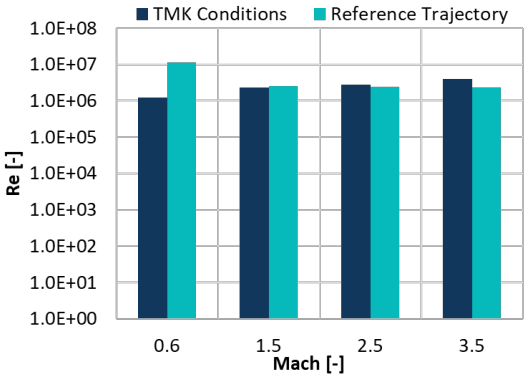

Fig. 6: RETALT2 comparison of Reynolds numbers in TMK tests and in flight

3. RETALT1: AERODYNAMIC PHASE - TMK

As shown in Fig. 1 different aerodynamic control surfaces were tested for RETALT1 for the aerodynamic phase. Namely, interstage segments (petals), depicted in Fig. 1a, planar fins, shown in Fig. 1b and c, and grid fins.

The test results with the petal configuration were discussed in detail in [4], were also the test methodology and setup were reported in detail. Here complementary, to those results the results with planar fins shall be the focus of this section. The RETALT1 wind tunnel model with planar fins mounted in the TMK is shown in Fig. 7. It was equipped with an in-house DLR six components strain gauge balance for force and moment measurements. Fig. 8 shows the profile of the planar fins.

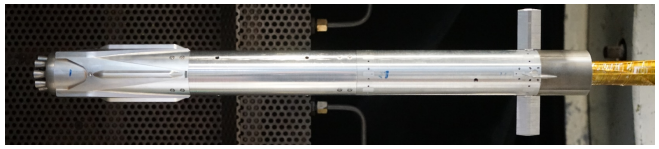

Fig. 7: RETALT1 TMK wind tunnel model with planar fins mounted in TMK.

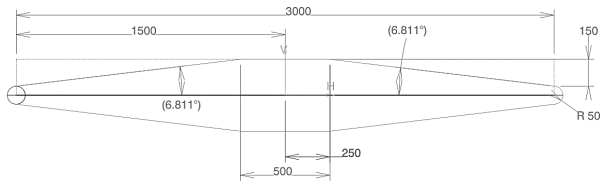

Fig. 8: Profile of planar fins of RETLAT1 [4]

It was discussed in [4], that applying the blast wave analogy [8], it can be reasoned that the free stream conditions at the ACS can be estimated with the total pressure downstream of a normal shock and the static pressure of the free stream.

Furthermore, it was observed that the pressure at the ACS follows a negative modified Newtonian law:

$$C_{p_{Newton\,min}} = -C_{p_{max}} \sin^2 \alpha \qquad (1)$$

Where, $C_{p_{Newton\,min}}$ is the pressure coefficient at the ACS, $C_{p_{max}}$ is the pressure coefficient of the total pressure downstream of a normal shock and α is the angle of attack. This correlation can be observed in Fig. 9, taken from [4], where Cp11, and Cp13 are the pressure coefficients close to the ACS, which follow the dotted black line depicting the negative modified Newtonian law, up to angles of attack of about $\pm 7°$.

In [3] the flow conditions at the ACS were estimated with this approach to analytically size the planar fins with the aid of oblique shock relations and Prandtl-Meyer expansion relations.

This approach of sizing the planar fins shall be assessed in the following. For that, the measured data of the plain configuration of RETALT1 without any control surfaces (B0,0,0,0) is superimposed with the planar fins. The results are then compared to the measured data of the planar fin configuration (PF0,0,0,0).

In Fig. 10 the normal force coefficient is shown. The blue line represents the plain configuration. The black line shows the measured planar fin data. The symbols show three analytical approaches. The squares show the planar fins calculated with oblique shock relations. However, due to the blunt leading edge of the fins (see Fig. 8), the stream lines close to the surface pass a normal shock upstream of the leading edge before running along the surface. Therefore, the black triangles show the corrected approach of estimating the pressures on the surface of the fins by assuming the total pressure downstream of a normal shock but the static pressure passing thought an oblique shock. It is observable, that this data fits the measured data better. For the white triangles the static pressure at the ACS was corrected with the negative modified Newtonian law described above. With this correction the superimposed CN fits the measurements very well for angles of attack up to $\pm 8°$. For higher angles of attack the method seems to underestimate the CN. This is reasonable as for angles of attack higher than $\pm 7°$ the negative modified Newtonian law does not hold anymore as visible in Fig. 9. In Fig. 11 the pitch moment coefficient around the center of gravity (CM(CoG)) resulting with the superimposed CN is shown. As for the CN up to angles of attack of $\pm 7°$ the CM(CoG) is well approximated with the analytical method for the fins, for higher angles of attack it tends to deviate.

Fig. 12 shows the CM(CoG) for various fin deflections. For a deflection of the fins, the assumptions taken in the analytical approach are less valid, as the fins see more complex free stream conditions. The analytical method generally overestimates the efficiency of the fins, even though the general trend of the CM(CoG) is captured well.

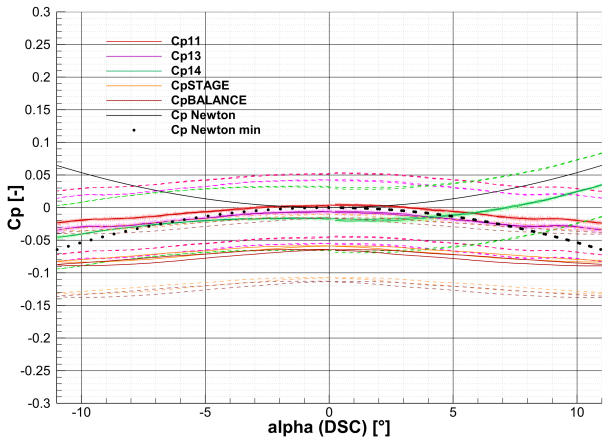

Fig. 9: Pressure coefficients close to the ACS for Mach 3.5 taken from [4] (Cp11, Cp13 – pressure coefficients close to the ACS) (dashed lines show measurement uncertainties)

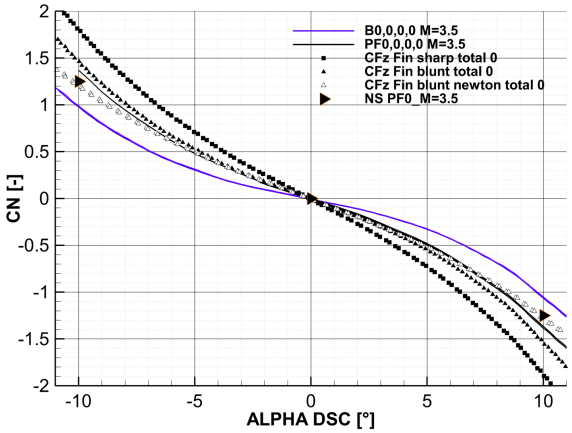

Fig. 10: Comparison CN for superimposed planar fins with measured planar fin configuration with $\delta = 0°$

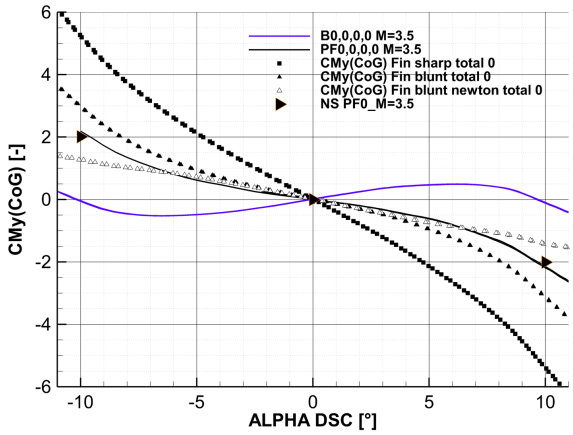

Fig. 11: Comparison CM(CoG) for superimposed planar fins with measured planar fin configuration with $\delta = 0°$

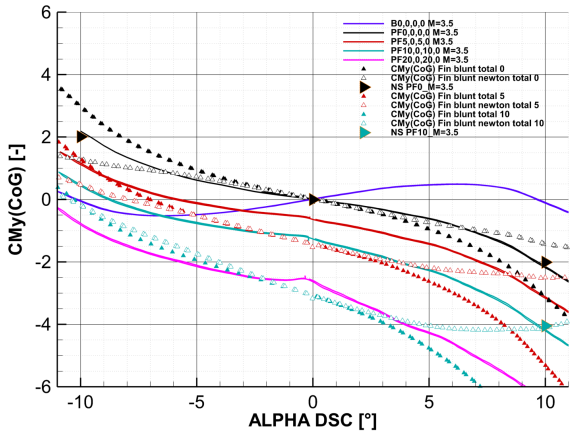

Fig. 12: Comparison CM(CoG) for superimposed planar fins with measured planar fin configuration for several deflection angles

4. RETALT2 AERODYNAMIC PHASE – TMK

As mentioned in the introduction, the aerodynamic phase of the RETALT2 configuration was tested in the Trisonic Wind Tunnel Cologne (TMK). The TMK is a blow down facility. Air from a high-pressure reservoir (up to 60 bar) passes a storage heater and is accelerated to supersonic Mach numbers in an adjustable Laval nozzle. In the subsonic regime, the Mach number is set with the aid of a diffusor downstream of the test section. The Mach numbers that can be tested in the TMK range from 0.5 up to 4.5, or up to 5.7 with the use of an ejector. The wind tunnel has a rectangular 60 cm x 60 cm test section.

The dimensions of RETALT2 are shown in Fig. 13. The wind tunnel model was scaled by a factor of 1/105. The RETALT2 wind tunnel model mounted in the TMK is shown in Fig. 14. The model design is depicted in Fig. 15.

Forces and moments were measured with a DLR six components strain gauge balance. The aerodynamic control surfaces of RETALT2 are deflected interstage segments, called petals. The deflection of the petals could be set by exchangeable ACS segments (yellow parts).

The reference frame of RETALT2 is shown in Fig. 16. The deflection of the petals was defined relative to its closed position ($\delta = 0°$). The origin of the reference frame was positioned in the tip of the closed configuration.

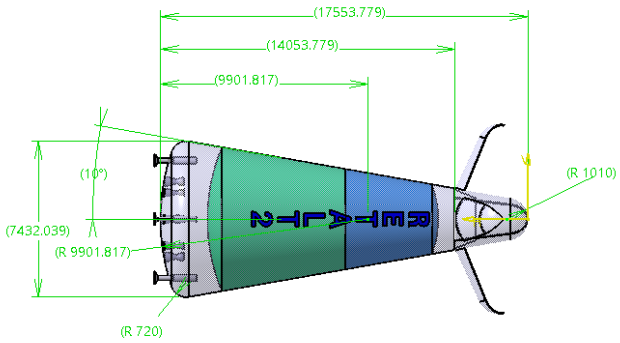

Fig. 13: Dimensions of RETALT2 flight configuration (in mm)

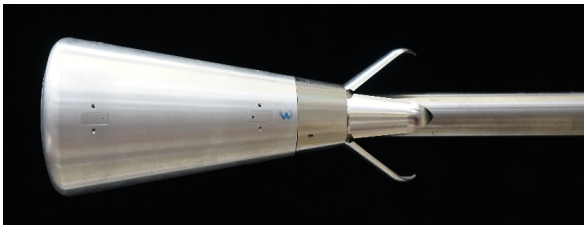

Fig. 14: RETALT2 wind tunnel model mounted in TMK

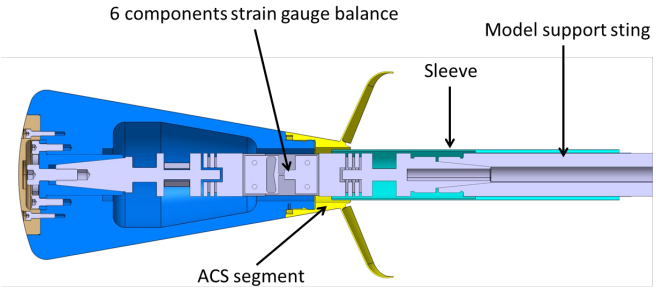

Fig. 15: RETALT2 model design with 6-components strain gauge balance

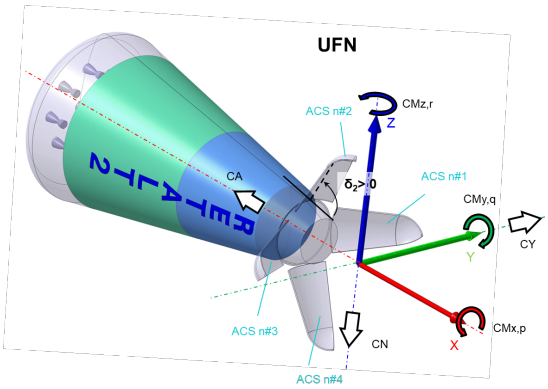

Fig. 16: RETALT2 reference frame

For the RETALT2 configuration a strong hysteresis effect was observed in the flow filed and, hence, also in the moment and force coefficients. The effect was strongest for the tested Mach number of 1.5. The moment coefficient around the center of gravity (CoG) at $X_{CoG} = -13.15$ m (flight scale) is shown in Fig. 17, the axial force coefficient is shown in Fig. 18. The coefficients are shown for several petal deflection angles (0°, 20°, 45°, 75°), where all petals were deflected equally.

At low angles of attack an attached flow configuration can be observed. This is shown in Fig. 19 on the left for a Mach number of 1.5, a deflection of $\delta = 45°$ and an angle of attack of 5°. The free stream passes a bow shock upstream of the vehicle and expands around the shoulders. It is recompressed along the conical body. Upstream of the petals a small recirculation region can be observed which leads to a separation shock. However, at high angles of attack the flow separates. Presumably due to a larger recirculation region in front of the petals. The flow separation leads to large jumps in the moment and axial force coefficients. For the case of Mach 1.5 and a petal deflection of 45° this can be observed at an angle of attack of about 10°. When the polar is running down again, the flow stays separated before it reattaches at low angles of attack of about ±2°. The separated flow case is shown in Fig. 19 on the right for the same angle of attack of 5° as the attached flow filed. For the polar to negative angles of attack flow separation occurred already at -9°. For a deflection of 45° also at low angles of attack the separated flow field could be observed (between 0° and 2°) as after the wind tunnel start this flow field occurred, before it reattached at about 2° for the up-running polar.

For lower deflection angels than 45° the hysteresis occurs at larger absolute angles of attack. It is interesting to note that for the deflection by 20° and 0° the hysteresis was only observed for negative angles of attack. A reason could be an effect of the sting or imperfections in the symmetry of the model. At a deflection of 75° no hysteresis was observed as only the separated flow case occurred. Rebuilding the hysteresis effect with CFD is challenging and strongly depends on the applied turbulence modelling. An analysis of this effect with CFD is discussed in [11].

For the trim of the vehicle only the upper petal was deflected. For these cases the hysteresis only occurred for the negative angle of attack polar, which is to be expected, as for this part of the polar the upper petal is on the windward side. [7]

As observed for the RETALT1 configuration in [4], also for RETALT2 large deflections of all petals lead to a stable configuration. For Mach 1.5 a deflection of 45° is necessary to reach trimmabiliy around 0° angle of attack (see Fig. 17). However, the deflection of only one petal does not lead to trimmable configurations close to 0° [7].

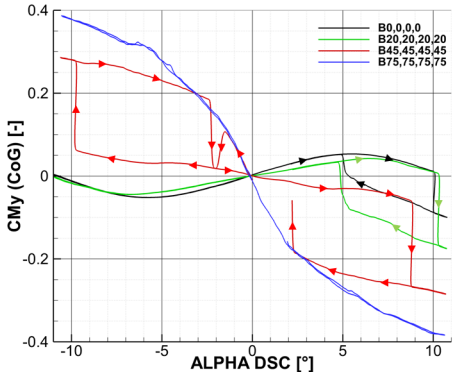

Fig. 17: Moment coefficient around the center of gravity (CoG) for Mach 1.5 for several petal deflections (all petals deflected equally)

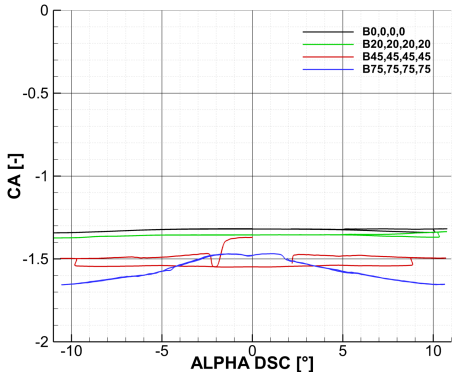

Fig. 18: Axial force coefficient for Mach 1.5 for several petal deflections (all petals deflected equally)

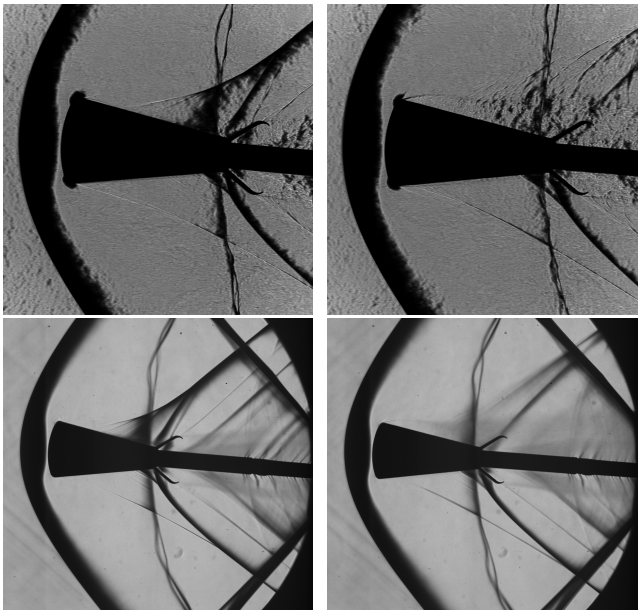

Fig. 19: Schlieren images at Mach 1.5 and at 5° angle of attach for up-running (left) and down-running (right) polar from high speed schlieren camera (upper images) and high-resolution camera (lower images)

5. RETALT1 LANDING PHASE – VMK

The landing phase of RETALT1 is rebuild in the Vertical Free-Jet Facility Cologne (VMK). The VMK is a blow down facility with an open test section. It is capable of simulating sea level conditions at Mach numbers up to 2.8. The wind tunnel model mounted in the test section is shown in Fig. 20.

The model is prepared to be tested with oxygen and hydrogen combustion in an internal combustion chamber in the wind tunnel model. However, in a first test series is was tested with high pressure air. The model nozzle contour was designed with an expansion ratio of 5.5.

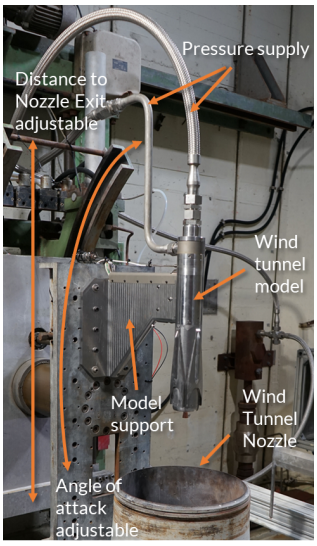

Fig. 20: RETALT1 wind tunnel model mounted in VMK

The supersonic jet exhausting into the free stream showed strong unsteady behavior. In Fig. 21 snapshots of highspeed schlieren videos with a frame rate of 25 kHz and an exposure time of 1.43 μs are shown for Mach 0.9, 0.8, and 0.7 at an ambient pressure ratio of $p_e/p_\infty = 0.704$. It can be observed that for higher Mach numbers the plume length gets shorter. Furthermore, for Mach 0.7 the variance of the Schlieren images over 200 images is shown. The highest variance is visible in the stagnation region where the plume meets the free stream as here the fluctuations are the largest.

An analytical formulation for the estimation of the plume length x normalized with the nozzle exit diameter D_e was defined in [12]:

$$\frac{x}{D_e} = 3.1\left(\frac{\rho_e u_e^2}{\rho_\infty u_\infty^2}\right)^{\frac{1}{2}}\left(\frac{T_{CC}}{T_e}\right)^{\frac{1}{2}} \qquad (2)$$

Where ρ_e, T_e and u_e are the density, the temperature and the velocity at the nozzle exit, T_{cc} is the total pressure in the combustion chamber and, ρ_∞ and u_∞ are the density and velocity in the free stream. Hence, the plume length depends on the temperature ratio of the expansion in the nozzle and on the momentum flux ratio of the jet flow at the nozzle exit with the free stream. It can be noted that regarding this formulation the plume length follows a linear trend with square root of these two ratios, with a factor of 3.1. In Fig. 22 the plume length was extracted from the schlieren videos for several ambient pressure ratios and was plotted against the right side of equation (2). The linear dependency of the plume with these ratios can be confirmed. However, the factor found for the fitting of the data was 2.57 instead of 3.1 as reported in [12].

This is a good indication that besides the ambient pressure ratio, the momentum flux ratio and the temperature ratio of the total and the exit temperature of the nozzle are important similarity parameters to be considered in the experimental rebuilding of the landing burn. Furthermore, this relation can be helpful for the design of such experiments. As the necessary distance of the model nozzle exit to the wind tunnel nozzle exit can be estimated.

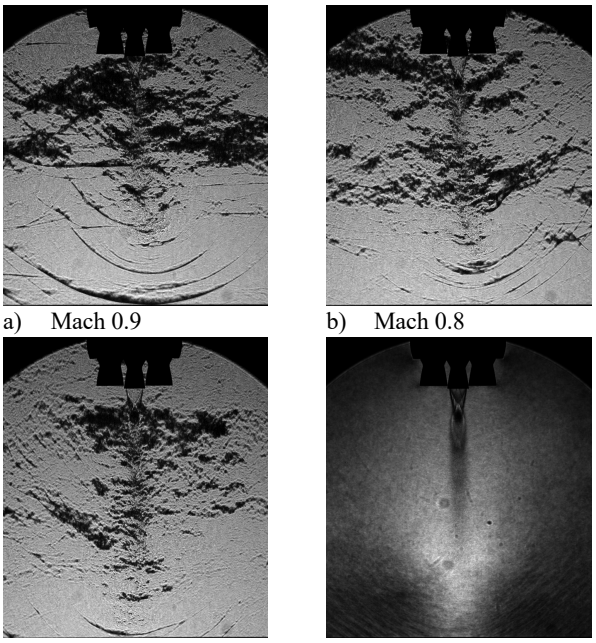

a) Mach 0.9 b) Mach 0.8

c) Mach 0.7 d) Variance at Mach 0.7 over 200 schlieren images

Fig. 21: Snapshot of highspeed schlieren videos (a, b, c) and variance in the flow field (d) for an ambient pressure ratio of $p_e/p_\infty = 0.704$

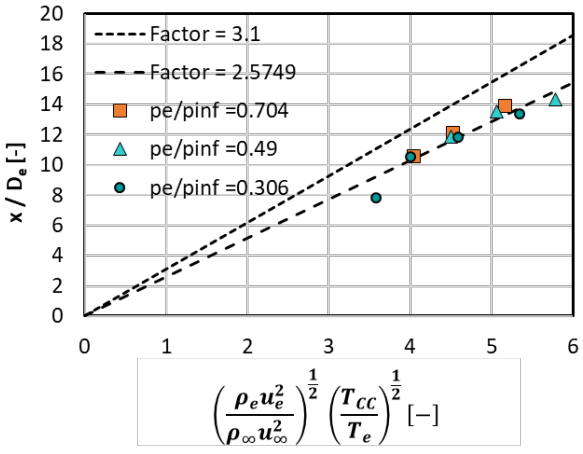

Fig. 22: Comparison of analytical formulation with measured plume length

6. RETALT1 RE-ENTRY BURN – H2K

The re-entry burn of the RETALT1 vehicle was tested in the Hypersonic Wind Tunnel Cologne (H2K) the test and model setup were described in detail in [9], where the retro propulsion maneuver for a single engine and for three engines was analyzed in detail regarding their steady flow characteristics. A comparison of the wind tunnel test results with CFD computations was presented in [10].

The H2K is a blow down wind tunnel from high pressure air (up to 60 bar) down to vacuum. Mach numbers from 4.8 up to 11.2 can be reached in the wind tunnel. The exit diameter of the wind tunnel nozzle is 60 cm. The RETALT1 wind tunnel model mounted in the H2K is shown in Fig. 23.

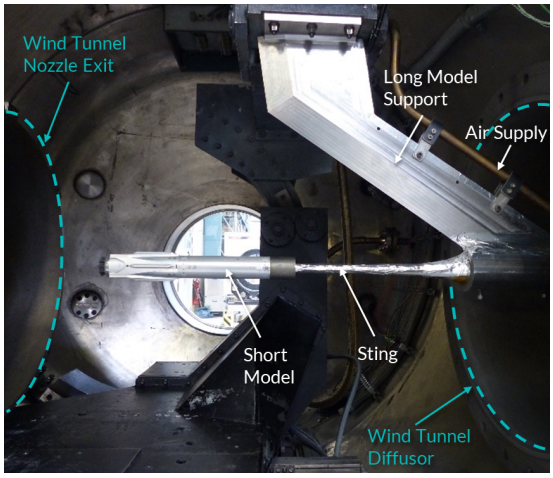

Fig. 23: RETALT1 wind tunnel model mounted in H2K [9]

For the understanding of the unsteady behavior of the flow field the variance in the schlieren images is shown for the case with three active engines at a Mach number of 5.3 and a thrust coefficient of 2.29 in Fig. 24. Fig. 24a shows a snapshot of the long penetration mode described in [9]. The variance computed over 400 images is shown in Fig. 24b. It is clearly visible that the complete bow shock area is fluctuating mainly upstream of the termination shocks formed by the three plumes. Fig. 24c and Fig. 24d show the variances over only 10 images, for the long penetration mode and the blunt mode. These images show that even though the flow flied seems to settle in one of the modes for some time, the general flow structure still shows large fluctuations.

The question arose weather these fluctuations are also visible in the pressure measurements in the base area. Therefore, a spectrogram of the pressure measurements over the thrust coefficient was computed and is shown in Fig. 25 for the sensors 331, 311 and 322. It was found that mainly for the pressure sensors very close to the center nozzle dominant frequencies could be found at 22.6 kHz, 21.9 kHz and 21.1 kHz. As these frequencies seem to be relatively independent of the thrust coefficient they could be more related to the exit plume than to the counterflow environment. However, it can be observed that their power spectral density (PSD) slightly increases with increasing thrust coefficients. In the other sensors these dominant frequencies were not observed, as can be seen for 322 in Fig. 25. Furthermore, a dominant frequency around 2.5 kHz was found (Fig. 25) which correspond well with [13]. Who found a dominant frequency of about 2 kHz in Schlieren images of retro propulsion flow fields with a single active engine. However, for the three engines case the higher frequencies are more dominant than the lower frequency of 2.5 kHz. Modal analyses of the Schlieren images shall be performed in the future to gain a more thorough understanding of the underlying physical phenomena of the occurring frequencies.

Frequency analyses of Schlieren images of such retro propulsion configurations with three active engines tested in the H2K were performed in the RETPRO project and are presented in [14].

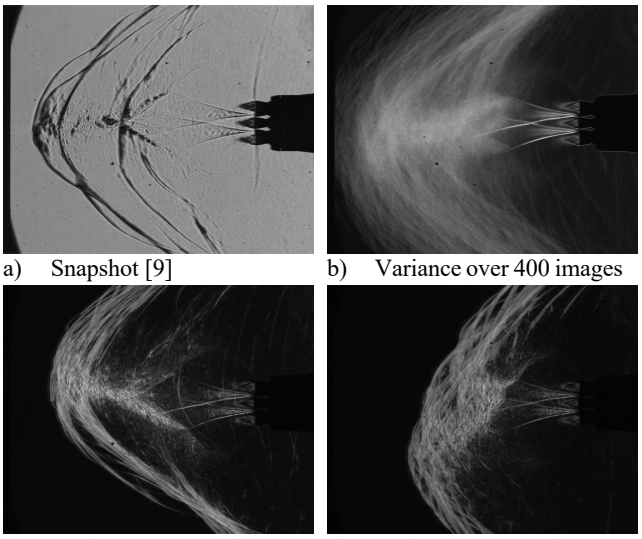

a) Snapshot [9] b) Variance over 400 images

c) Variance over 10 images of long penetration mode d) Variance over 10 images of blunt mode

Fig. 24: Variance in schlieren images recorded at a frame rate of 20 kHz for $M_\infty = 5.29, C_T = 2.29 \pm 0.13, T_{CC} = 300\text{K}, p_0 = 4\text{ bar}, T_0 = 450\text{ K}$

7. CONCLUSION

In this paper the flight phases of vehicles descending and landing with the aid of retro propulsion have been analyzed, focusing on specific findings for the various flight phases of RETALT1 and RETALT2 in the wind tunnel experiments.

In the aerodynamic phase of RETAL1 it was found that the flow conditions at the aerodynamic control surfaces can be well approximated with the analytical procedure proposed in [4] and with the aid of oblique shock relations and Prandtl-Meyer expansion relations.

For RETALT2 a strong hysteresis effect was found resulting from a flow separation due to a recirculation region upstream of the petals.

For the landing burn of RETALT1 it was found that the momentum flux ratio and the temperature ratio of the total temperature in the combustion chamber and the temperature at the nozzle exit are important similarity parameters to be considered for such configurations as they dominate the plume length and hence the flow field besides the ambient pressure ratio.

In general, highly unsteady flow fields are observable for the landing and the re-entry burn which can be seen in a large variance in the

flow field. These can lead to dominant frequencies as shown for the re-entry burn of RETALT1.
In future work the unsteady behavior of these retro propulsion flow fields shall be analyzed further, as the understanding of the possibly resulting pressure loads can be critical for the design of structural components.
Furthermore, the effect of the combustion of oxygen and hydrogen on the landing burn and the resulting pressure and heat loads on the vehicle will be tested in the VMK in the near future.

ACKNOWLEDGMENTS

The RETALT project has received funding from the European Union's Horizon 2020 research and innovation framework program under grant agreement No 821890.
The authors also want to thank the H2K, TMK and VMK team. Without their effort, expertise and passion acquiring the data presented in this paper would not have been possible.

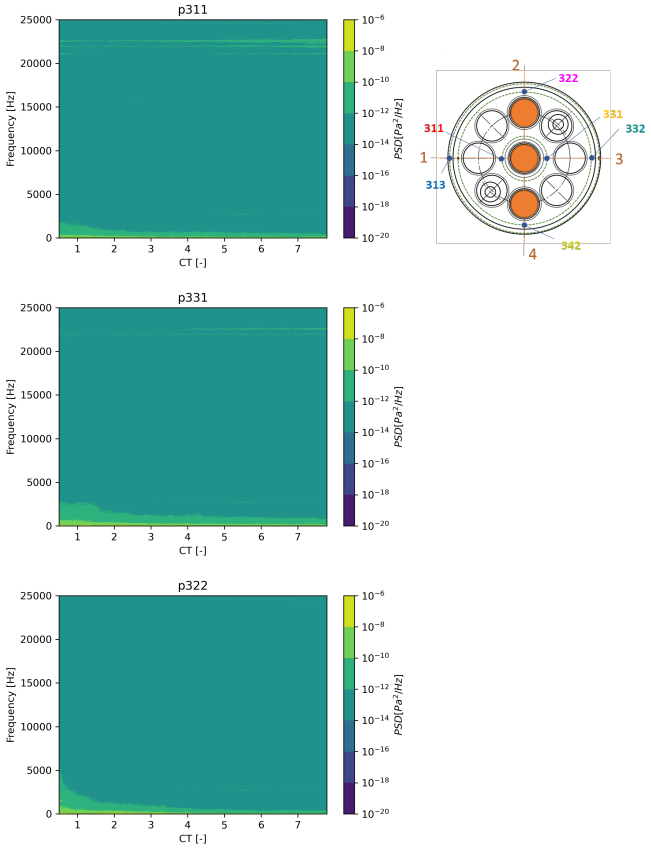

Fig. 25: Spectrograms of pressure measurements on the base area of RETALT1 versus the thrust coefficient, for 3 active engines and $M_\infty = 5.29, T_{CC} = 300\text{K}, p_0 = 4\text{ bar}, T_0 = 450\text{ K}$

REFERENCES

[1] Marwege, A.; Gülhan, A.; Klevanski, J.; Riehmer, J.; Kirchheck, D.; Karl, S.; Bonetti, D.; Vos, J.; Jevons, M.; Krammer, A.; Carvalho, J.: „Retro Propulsion Assisted Landing Technologies (RETALT): Current Status and Outlook of the EU Funded Project on Reusable Launch Vehicles", 70th International Astronautical Congress (IAC), Washington D.C., United States, 21-25 October 2019.

[2] Marwege, A.; Klevanski, J.; Hantz, C.; Kirchheck, D.; Gülhan, A.; Karl, S.; Laureti, M.; De Zaiacomo, G.; Vos, J.; Thies, C.; Jevons, M.; Krammer, A.; Lichtenberger, M.; Carvalho, J.; Paixão, S.: „Key Technologies for Retro Propulsive Vertical Descent and Landing – RETALT – an Overview", 2nd FAR conference, 19–23 June 2022, Heilbronn, Germany.

[3] Marwege, A.; Gülhan, A.; Klevanski, J.; Hantz C.; Karl, S.; Laureti, M.; De Zaiacomo, G.; Vos, J.; Jevons, M.; Thies, C.; Krammer, A.; Lichtenber, M.; Carvalho, J.; Paixão, S.: "RETALT: Review of Technologies and Overview of Design Changes", CEAS Space J

[4] Marwege, A.; Hantz, C.; Kirchheck, D.; Klevanski, J.; Gülhan, A.; Charbonnier, D.; Vos, J.: "Wind Tunnel Experiments of Interstage Segments used for Aerodynamic Control of Retro-Propulsion Assisted Landing Vehicles", CEAS Space J (2022). https://doi.org/10.1007/s12567-022-00425-4

[5] Hantz, C.; Marwege, A.; Paixão, S.; Celotti, L.; Wisniewska, M.: "Thermal characterization of cork- and ceramics-based TPS in DLRs arc-heated wind tunnel", 2nd FAR conference, 19–23 June 2022, Heilbronn, Germany.

[6] Marwege, A.; Hantz, C.; Klevanski, J.; Gülhan, A.; Vos, J.; Charbonnier, D.: "RETALT1 – Aerodynamic Data Base 2.0", Zenodo, 2022, https://zenodo.org/record/6597913

[7] Marwege, A.; Hantz, C.; Klevanski, J.; Gülhan, A.; Vos, J.; Charbonnier, D.; Karl, S.: "RETALT2 – Aerodynamic Data Base 2.0", Zenodo, 2022, https://zenodo.org/record/6597972

[8] Sakurai, A., "On the Propagation and Structure of the Blast Wave II," Journal of the Physical Society of Japan, Vol. 9, March–April 1954, p. 256. https://doi.org/10.1143/JPSJ.9.256

[9] Marwege, A.; Kirchcheck, D.; Klevanski, J.; Gülhan, A.: "Hypersonic Retro Propulsion for Reusable Launch Vehicles Tested in the H2K Wind Tunnel", CEAS Space J (2022).

[10] Vos, J.B., Charbonnier, D., Marwege, A., Gülhan, A., Laureti, M., Karl, S.: "Aerodynamic Investigations of a Vertical Landing Launcher Configuration by means of Computational Fluid Dynamics and Wind Tunnel Tests", AIAA Scitech 2022 Forum, San Diego, 2022, https://zenodo.org/record/5814915

[11] Vos, J.; Charbonnier, D.; Marwege, A.; Hantz, C.; Gülhan, A.: "CFD Simulations and Wind Tunnel Experiments for Re-usable Launch Vehicles", 2nd FAR conference, 19–23 June 2022, Heilbronn, Germany.

[12] Jarvinen, P. O.; Hill, A. F.: "Penetration of Retrorocket Exhausts into Subsonic Counterflows", Journal of Spacecraft and Rockets, Vol 10, 1973, https://doi.org/10.2514/3.27737

[13] B. F., Bathel; C. R., Litzner; S. B., Jones; S. A., Berry; N. T., Smith; T. J., Garbeff: "High-Speed Schlieren Analysis of Retropropulsion Jet in Mach 10 Flow". Journal of Spacecraft and Rockets 57.1 (2020), pp. 33–48. https://doi.org/10.2514/1.A34522

[14] Kirchheck, D.; Marwege, A.; Klevanski, J.; Gülhan, A.: "Hypersonic Retrograde Propulsion Experiments – a basis for validation of CFD within RETPRO", EUCASS, 2022